Water heating control for efficiency enhancement of Proton Exchange Membrane Electrolyser using Photovoltaic panels and MPPT

A. Tabanjat[1], M. Becherif[1], M. Emziane[2], D. Hissel[3] and B. Mahmah[4]

[1]UTBM, FEMTO-ST/FCLab, UMR CNRS 6174, 90010 Belfort Cedex, FRANCE.
[2]Masdar Institute of Science and Technology, Abu Dhabi, UAE.
[3]UFC, FEMTO-ST/FCLab, UMR CNRS 6174, 90010 Belfort Cedex, FRANCE.
[4]CDER, Center of Development of Renewable Energy, BP 62,
Street of observatoire Bouzaréah; Algiers – Algeria
abdulkader.tabanjat@utbm.fr, mohamed.becherif@utbm.fr,
memziane@masdar.ac.ae, daniel.hissel@univ-fcomte.fr,
mah2bouziane@gmail.com

Keywords: Proton Exchange Membrane Electrolyser, Maximum Power Point Tracking, Fuzzy Logic, Photovoltaic.

ABSTRACT:

The studied system consists of a 59 kW Proton Exchange Membrane (PEM) electrolyser 6 powered by a photovoltaic (PV) generator through a boost converter for H_2 production. The PV panels were sized to 63 kW according to the Belfort region in France, and controlled using Maximum Power Point Tracking (MPPT) technique allowing the extraction of the maximum available power. It is also shown that the produced H2 flow is increased if the input water is heated. The optimal input water temperature is investigated in order to maximize the produced H_2 by taking into account the physical constraints when using a maximal temperature in a given system and the limitation to avoid the transformation of the water into vapor. Fuzzy Logic (FL) control is used to determine the instantaneous optimal water temperature and a simple proportional integral (PI) controller heats the inlet water to the optimal temperature. It is also shown that the pressure affects the system efficiency and temperature, and the proposed controller manages the water temperature and pressure. The proposed system design allows the production of H_2 and the extraction of the maximal available solar power. The electrolyser efficiency is substantially increased as a result of using MPPT for the PV panels and FL with PI as water heating controllers.

I- INTRODUCTION:

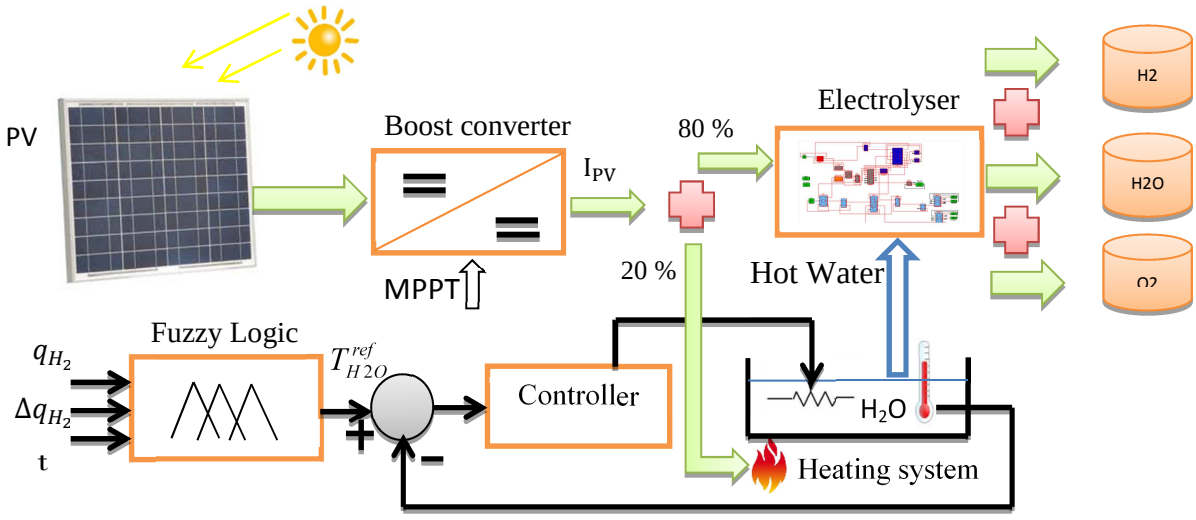

Fig. 1: The proposed system for the PV-Electrolyser with water heating control

Batteries bank can be a solution for energy storage, but their disadvantages are low energy density, self-discharge, leakage characteristics, and are not suitable for long-term energy storage. Hence, batteries are not the best solution [1]. Hydrogen can be stored for a long period with low energy losses and its quantity

increases with water temperature heating (Fig. 2). This makes hydrogen suitable for energy storage. Moreover, hydrogen is better suited where the conventional fossil fuel is expensive.

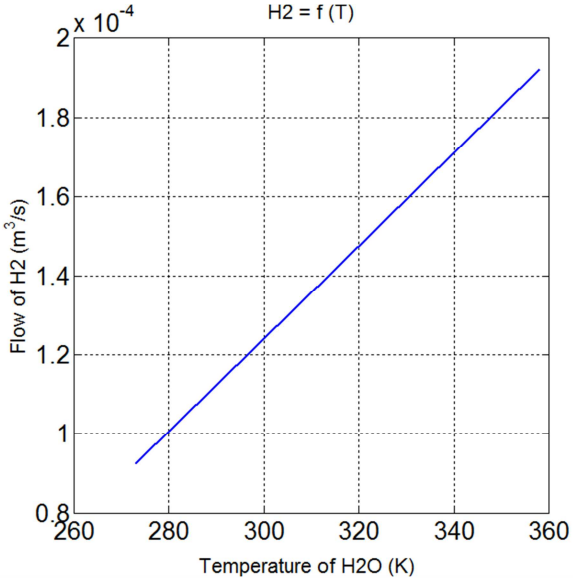

Fig. 2: Flow of H_2 versus water temperature

In the PEM Electrolyser, water is supplied through water pipes at the anode reaction interface [2, 3]. Oxygen is produced at the anode side and hydrogen is produced on the cathode side as explained in reaction (1) (Fig. 3) and (Fig. 4). The most commonly used membrane material is Nafion. It produces oxygen, protons and electrons by applying a DC voltage. At the cathode side, hydrogen is formed by the recombination of electrons and protons (2) (Fig. 3). The overall chemical reaction of the water electrolysis is given by (3).

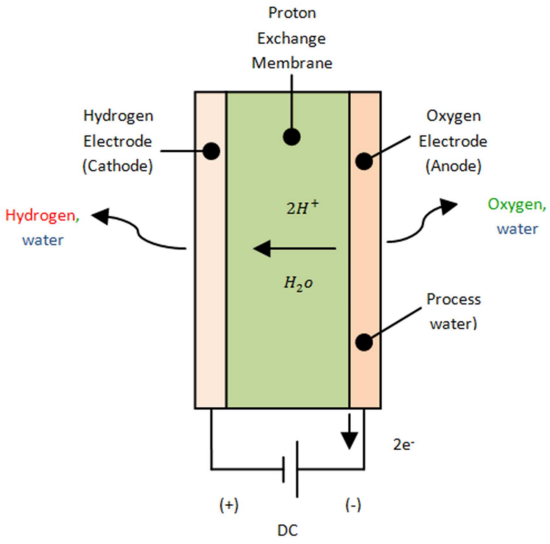

Fig. 3: Internal structure of a PEM Electrolyser [4, 5]

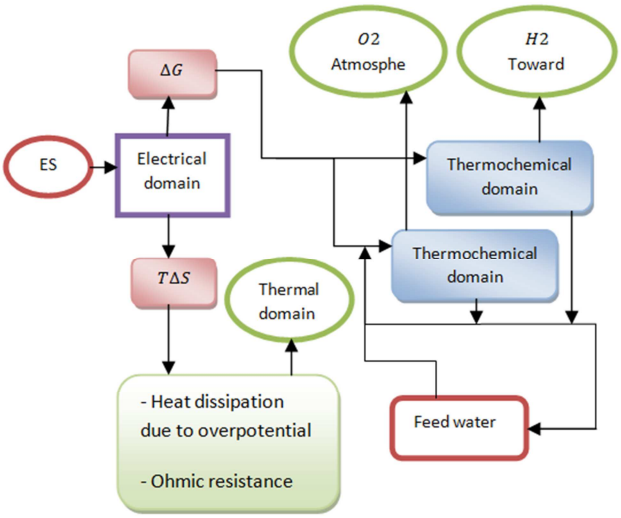

Fig.4: Physical interactions within an electrolyser [1, 5]

$$H_2O \rightarrow \frac{1}{2}O_2 + 2H^+ + 2e^- \quad (1)$$

$$2H^+ + 2e^- \rightarrow H_2 \quad (2)$$

$$H_2O \rightarrow \frac{1}{2}O_2 + H_2 \quad (3)$$

Reactions (1, 2 and 3) have to be decoupled into the different physical areas:

Three kinds of fluidic links in the electrolyser stack can be considered (Fig. 3):

- At first, on both anode and cathode inlets, liquid water is supplied, while the liquid water and the gas produced are removed from both outlets.

- In the second step, liquid water is only supplied to the anode inlet and at the anode and cathode outlets, liquid water and produced gases are collected.
- At the end, the feeding water is supplied to the anode inlet only, but at the outlet channels, the vapor water and the produced gas are drained off.

In Fig. 4, the synoptic of internal phenomena in the electrolyser is presented.

The energy produced by renewable energy sources (wind turbines and PV panels) are used in the electrolyser to split the water molecule into hydrogen and oxygen. This energy is supplied by applying DC voltage level between the stack terminals expressed by V_{ref} = ΔG/nF at the standard condition (T = 25 °C, p = 1 atm). At this voltage point, the heat energy needed is TΔS (S is the entropy and T the temperature) that must be taken from the surrounding environment [6], and the energy needed is expressed by the enthalpy ΔH = ΔG + TΔS. The voltage needed for splitting the water is: $V_{tn} = \Delta H/\,nF = 1.482\,V$.

For obtaining electrochemical energy and thermal energy, necessary heat energy covered partially or completely by the electrical energy. If partially the electrical energy needed to convert chemical energy is taken from the electrolyser environment if the heat of electrolyser is not enough. In the Fig. 4, energy flows are represented by the arrows.

Two kinds of PEM electrolysis are considered: low-pressure water electrolysis below 30 bars and high pressure water electrolysis above 30 bars up to 135 bars.

The electrolyser efficiency does not exceed 75% and that of Fuel Cell (FC) system does not exceed 40%, so the overall efficiency of total system is about 27%, which is low compared to the batteries. On the other hand, the battery self-discharge makes it unable to consider long storage periods.

I.I Short presentation of the considered graphic modeling tool:

The Energetic Macroscopic Representation (EMR) is an energy-based graphical modeling tool to describe complex electrochemical systems. It is based on the action-reaction principle to organize the interconnection of subsystems according to the physical causality (i.e. integral causality). The inversion of the graphical description by using specific rules leads to a Maximal Control Structure (MCS) of the system for which it is assumed that all variables are measurable. This methodology has been successfully applied to fault-tolerant supplies, railway traction systems, wind energy conversion systems, hybrid electric vehicles using super-capacitors [7] and energy storage systems using compressed air [8]. Thus, it has been possible to extend EMR beyond its initial aims in order to describe all multi-physics systems [9, 10]. Practical Control Structure (PCS) can be deduced from the MCS by applying simplification rules and using only few available measurements. More details can be found in [9], [10], [11], [12] and [13].The principal blocks of EMR are explained in [14].

I.II Short presentation of fuzzy logic controller:

This type of control approaches the human reasoning and makes use of the tolerance, uncertainty, imprecision and fuzziness in the decision-making process. It manages to offer a satisfactory performance without the need for a detailed mathematical model of the system, just by incorporating the experts' knowledge into fuzzy rules.

In addition, it has inherent abilities to deal with imprecise or noisy data; thus, it is able to extend its control capability even to those operating conditions where linear control techniques fail (i.e., large parameter variations).

This system has four main parts. First, using input membership functions, inputs are fuzzified, then based on inference rules, outputs are produced and finally the fuzzy outputs are defuzzified and applied to the main control system.

Fig. 5 shows inputs and outputs membership functions and inference rules used for water temperature control.

Where: Q (or q_{H_2}) represents the hydrogen flow;
DQ (or Δq_{H_2}) represents the differential H_2 flow;
t is the electrolyser operation work;
T represents the water temperature.

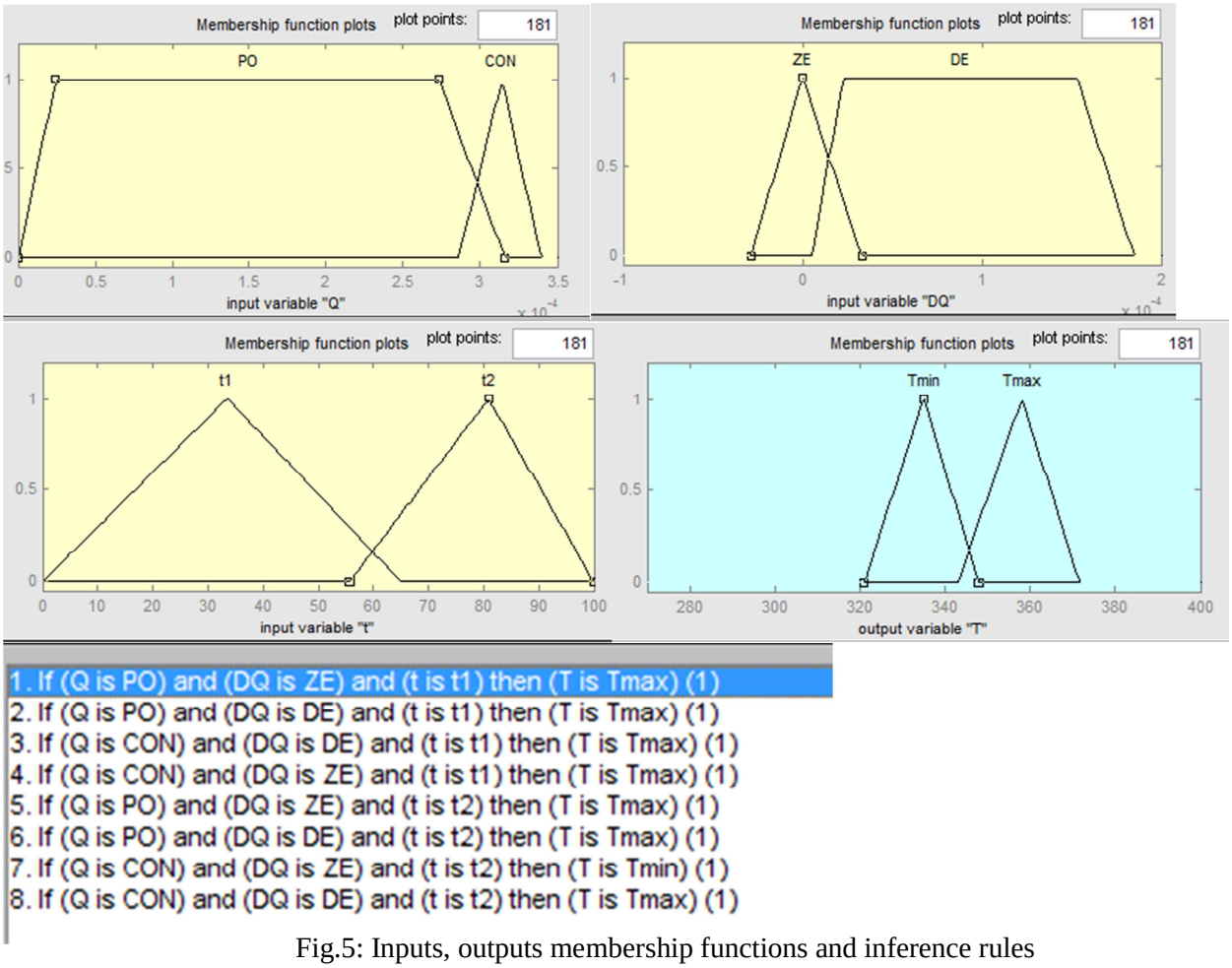

Fig.5: Inputs, outputs membership functions and inference rules

II- PV PARAMETERS DESCRIPTION:

The solar module is an association of n_{cells} cells in series with n_{cellp} cells in parallel [15], the conversion of solar energy into electrical energy is expressed by a non-linear relation between the current I_{PVm} and the voltage V_{PVm} of the module:

$$I_{PVm} = I_{phm} - I_{0m}\left[\exp\left(\frac{V_{PVm}+I_{PVm}.R_{sm}}{n.V_T}\right) - 1\right] - \frac{V_{PVm}+I_{PVm}.R_{sm}}{R_{shm}} \quad (4)$$

With: $V_T = \frac{KT_{PV}}{q}$

n	Ideality factor
$K\ [JK^{-1}] = 1.38 * 10^{-23}$	Boltzmann constant
q [C] = $1.602* 10^{-19}$	Electron initial charge
I_{PVm} [A]	The photo current
I_{0m} [A]	The diode saturation current
R_{sm} [Ω]	The serial module resistance
R_{shm} [Ω]	The parallel (shunt) module resistance

The photocurrent is related to the illumination by:

$$I_{ph} = \frac{E_e}{E_{ref}}\left(I_{ph,ref} + \mu_{ISC}\left(T_{PV} - T_{PV,ref}\right)\right) \quad (5)$$

E_e and E_{ref}	Irradiance at T_{PV} and the reference illumination.
$T_{PV,ref}$ [°C]=25	The temperature at standard test conditions (STC).

μ_{ISC} [A/K] The coefficient of variation of short-circuit current with respect to temperature (provided by the manufacturer).

II.I Maximum Power Point Tracking:

MPPT is a technique that inverters use to get the maximum possible power from solar panels. Because of complex relationship in solar cells between solar irradiation, temperature and total resistance, it produces a non-linear output I-V curve (Fig. 6). The aim of MPPT is to obtain and maintain a PV operating at the maximum power point, using MPPT algorithm [17].

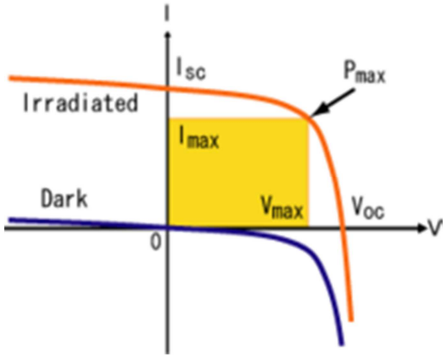

Fig. 6: V-I characteristics of a solar cell at a particular light level, and in darkness. [16]

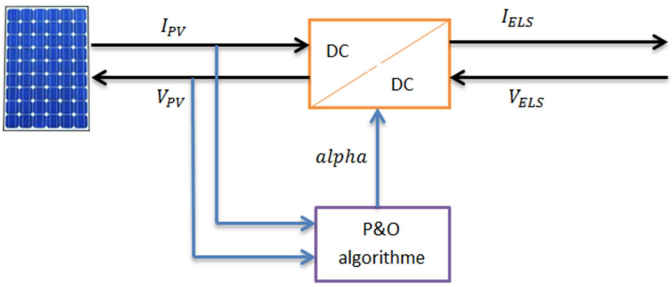

Fig. 7: Synoptic of PV panel and the boost converter controller using

For this purpose grid-tie inverters, solar battery chargers and similar devices are typically integrated into an electric power converter system that provides voltage or current conversion, filtering, and regulation for driving the electrolyser.

Many MPPT algorithms can be found [18]:

- Perturb and observe (P&O)
- Incremental conductance (IC)
- Parasitic capacitance (PC)
- Constant Voltage (CV)

In this PV model, MPPT P&O algorithm is chosen for its simplicity, robustness and ease of implementation (Fig. 7).

The module used for this purpose is TOTAL ENERGIE TE850 of 90 Wp (18V/5A).

Current-voltage and power-voltage curves of this PV module are shown in fig.8 for different solar levels (1000, 900, 800, 700, 600, 500 and 400) W/m²:

In this study, the solar irradiance is 1000 W/m² and the ambient temperature is of 25 °C

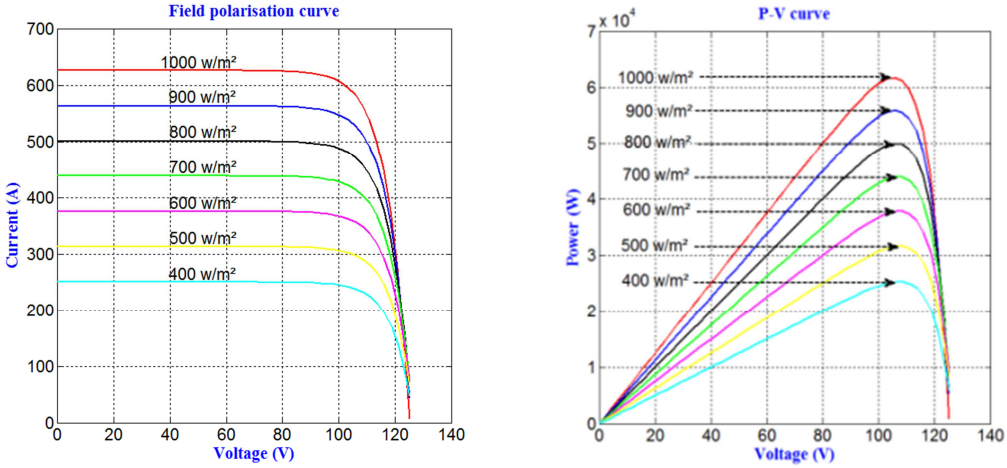

Fig. 8: I-V and P_V curves under different irradiance levels

III- ELECTROLYSER PARAMETERS DESCRIPTION:

The electrolyser used is staXX7 of H-TEC (59 kW, 300A), with an active area of 16 cm² and a membrane thickness of 130 µm. In the experimental test applied in FEMTO-ST laboratory the temperature is not controlled and the voltage is imposed and the current is obtained. The electrolyser parameters are given in [1]

The general PEM model blocks are constructed using EMR blocks (Fig.9):

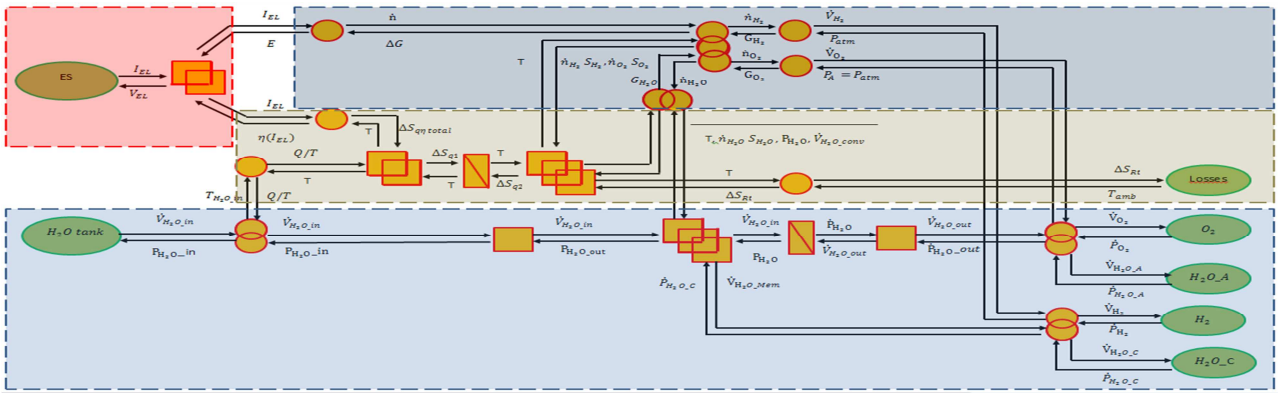

Fig.9: The General EMR construction of PEM electrolyser

IV- MAIN WORK:

Two approaches are used for a comparison purpose:

1 -With control of the water temperature.

2 – Without water temperature control.

The last assembly (Fig.10) comprises a voltage generator, the current shunt assembly for the regulation of the assembly and an oscilloscope for data acquisition.

IV.I Simulation of the model without water temperature control:

The temperature of the stack is measured by introducing two thermocouples in the two channels of the cathode evacuation. The tank temperature is measured with a third thermocouple which is introduced into the water tank.

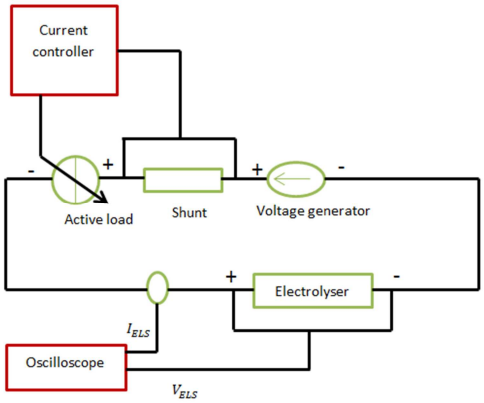

Fig. 10: The practical circuit [1]

IV.I.I The electrochemical parameters:

They are determined by identifying the parametric equation:

$$\dot{Q}_{H_2O\_Mem} = \dot{m}_{H_2O\_Mem}\, C_P (T - T_{amb}) \qquad (6)$$

This identification task is made using:

- A polarization curve.
- A free variation of the temperature during the drawing of the polarization curve.

$$V_{EL} = E + \eta_{El} + R_e j \qquad (7)$$

The five electrochemical parameters ($\alpha_A, \alpha_C, j_{0,A}, j_{0,C}, \sigma$) for equations η_{El} (activation over potential) determined through Matlab parameter identification tools (Lookup table) because these parameters are related to the operating temperature and there is no mathematical method to calculate them (Fig. 11).

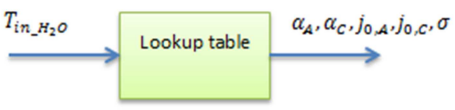

Fig. 11: $\alpha_A, \alpha_C, j_{0,A}, j_{0,C}, \sigma$ deduced by using Lookup table

α_A: Anode charge transfer coefficient

α_C: Cathode charge transfer coefficient

$j_{0,A}$: Anode exchange current density, A/cm²

$j_{0,C}$: Cathode exchange current density, A/cm²

σ: Membrane conductivity, s/cm

Using the following V-I curves (Fig. 12) the electrochemical parameters can be determined, for each of curve five values for five electrochemical parameters can be determined an so on for the other curves for goal of having a large scale of values determined at different temperature operating.

IV.I.II The thermal capacity of the stack C_{th_stack} and caloric capacity of the water tank $C_{tank\_H_2O}$:

The use of electrochemical parameters and thermal parameters enables obtaining the thermal capacity of the stack C_{th_stack} and caloric capacity of water tank $C_{tank\_H_2O}$ thanks to a heuristic approach consisting of scanning a range of incremental values in which the solution according to a priori physical knowledge of the system can be obtained.

IV.II Simulation with tank water temperature control:

Considering the temperature $T_{in\_H_2O}$ [° C] = (25, 30 ..... 50, 55, 60) and the potential values E [V] = $(E_{25\,°C}, E_{30\,°C} \ldots\ldots E_{50\,°C}, E_{55\,°C}, E_{60\,°C})$, and after that, the values of parameters $\alpha, \beta, \gamma, \delta, \upsilon$ of the equation $E_0 = \alpha + \beta T + \gamma T^2 + \delta T^3 + \upsilon T \ln T$ are determined using Matlab « Fittype » and « Cfit » for at the end finding the equation $E = E_0 + \Delta E$ with $\Delta E = \frac{RT}{2F} \ln (P_{H_2} P_{O_2}^{0.5})$. With the help of «Lookup table » of Matlab the electrochemical values are verified.

$$V_{EL} = E + \eta_{El} + R_e j \qquad (8)$$

V- SIMULATION RESULTS AND DISSCUSSION:

To obtain different curves of U=f (I) at different temperatures, the current is injected and the obtained voltage represent the result of electrolyser modeling.

The voltage curves as a function of the current at different temperature in the electrolyser are given by Fig. 12.a.

The electrolyser voltage was fixed at 200V and for each temperature curve, the current value is obtained as shown in Fig. 12.b:

Fig. 12.a

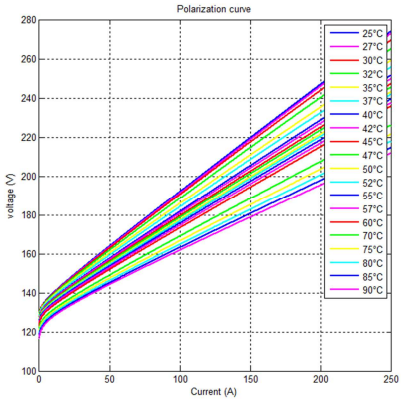

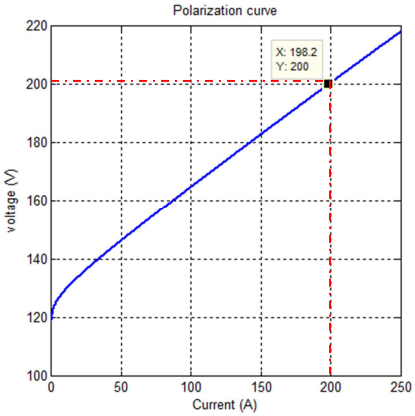

Fig. 12.b

Fig. 12.a: Polarization curve with different water temperature and Fig. 12.b: polarization curve at 80 °C.

The current at different temperatures are listed in Table 1:

Table 1: The current values as a function of temperature

I (A)	115.3	116.6	117.2	121.4	127.9	132.1	138.3	140.8	144.2	146.9
T (°C)	25	27	30	32	35	37	40	42	45	47
I (A)	150.4	152.7	156	159.5	163.5	179.9	190.1	198.2	206.1	213.6
T (°C)	50	52	55	57	60	70	75	80	85	90

These values are introduced into a Lookup table to obtain the current values as a function of temperature (Fig. 13).

The changes in water temperature cause changes in the electrolyser current and consequently changes in the hydrogen flow. Hence the hydrogen generation can be maximized through a water temperature control.

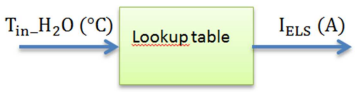

Fig. 13: Using Lookup table to obtain the PEM electrolyser current as function of water temperature

The curve of the hydrogen flow as function of the water temperature is given in Fig. 2 and the whole system (PV, electrolyser, MPPT, FL and PI controller) is given in Fig (1).

MPPT is used to maximize the output PV electric power while the water temperature control using PI controller maximizes the output electrolyser (H_2). FL technique is used to determine online the water temperature reference according to the physical constraints.

Firstly the model (PV and electrolyser) operates at a water temperature of 85 °C. However, this temperature threshold is not supported by the electrolyser during a long time period. Hence the FL technique decides to decrease this temperature reference after a specific period (that can be adjusted regarding a physical constraint) to a new threshold of 63 °C. After a "cooling" period of operation at low temperature, FL can increase once again the temperature reference and so on.

The primary source used for the water heating is obtained either by using unutilized long wavelength radiation received from the sun [19], or by subtracting part of the produced PV power, which represents about 20% of the whole PV power generated as depicted in Fig. 1. This second solution is applied in this work.

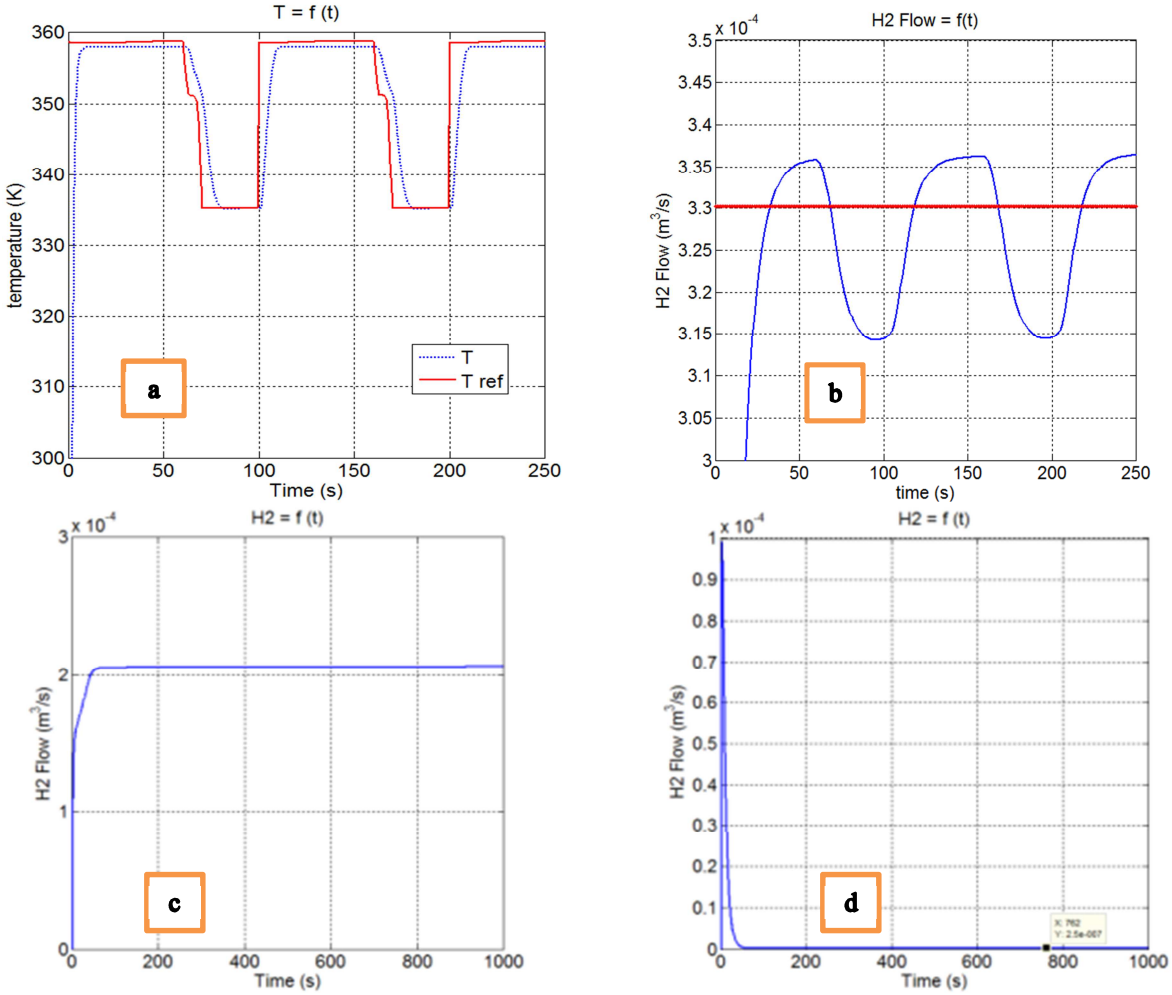

Fig. 14: Hydrogen flow at PEM Electrolyser with temperature control

In Fig. 14, the subfigs represent:
Control of water temperature with PV-MPPT; (a)

Electrolyser H_2 flow using water temperature control and MPPT; (b)
Electrolyser H_2 flow without water temperature control and with MPPT; (c)
Electrolyser H_2 flow without water temperature control and without MPPT; (d)

The electrolyser operation period at the maximal water temperature of 85 °C is equal to 2/3 of its total operation cycle and the average flow of hydrogen production in this case $3.302 * 10^{-4} \mathrm{m}^3/\mathrm{s}$. On the other hand, this flow is only $2.1 * 10^{-4} \mathrm{m}^3/\mathrm{s}$ when there is no water temperature control (i.e. with PV-MPPT) and the water temperature is 15 °C, so the increased amount of H_2 using the proposed control is:

$$\frac{3.302 * 10^{-4} - \ 2.1 * 10^{-4}}{2.1 * 10^{-4}} * 100 = 57.24\ \%$$

This result shows that the water temperature control is very important to increase the H_2 flow at the output, and the proposed control used is very powerful when combined with the PV-MPPT.

For the case where the MPPT control and water temperature control are not applied, the hydrogen flow decreases to a very low value, and its value of $2.5 * 10^{-7}\ m^3/s$.

A modification of the maximum water temperature threshold has to be considered for different geographic altitudes because of the ambient pressure changes. The boiling temperature changes with altitude, and a modification of the maximum temperature supported by the electrolyser has to reconsidered as explained in Fig. 15.

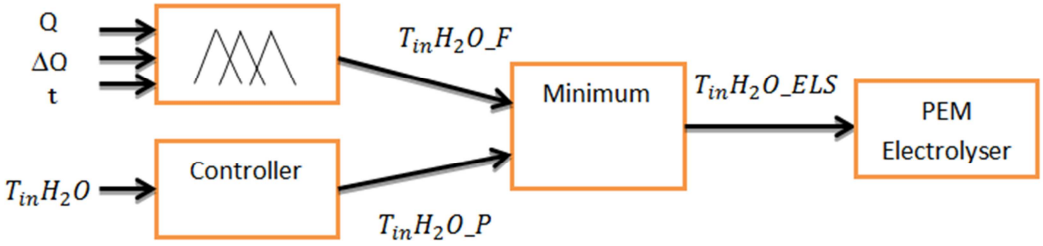

Fig. 15: The water temperature applied on the electrolyser after control it.

$T_{in}H_2O$	Electrolyser input water temperature
$T_{in}H_2O\_P$	Electrolyser input water temperature considering the pressure changes
$T_{in}H_2O$_F	Electrolyser input water temperature using water temperature FL controller
$T_{in}H_2O\_ELS$	Water temperature provided to PEM electrolyser

Any change in pressure will cause maximal temperature change and there will be a comparison between maximum water temperatures resulted from both mentioned controllers $T_{in}H_2O$_F and that of pressure controller $T_{in}H_2O\_P$. As a result, the minimum value between $T_{in}H_2O$_F and $T_{in}H_2O\_P$ will be taken as input for the PEM electrolyser.

VI- CONCLUSION:

In this article, the effect of the water tank temperature on the hydrogen flow is studied. The water temperature range studied is between 25 °C and 90 °C. The results show that the increase of water temperature improves the system efficiency, and that the hydrogen flow is proportional to the water temperature. In order to maximize hydrogen flow at the electrolyser output, a Fuzzy Logic controller is applied to maximize the water temperature and at the same time keep the maximum threshold temperature as long as possible, figs (14.a and 14.b). On the other hand, to maximize the power at the PV output, the MPPT method is applied. The result shows that, the comparison between the hydrogen flow in case of no control of water temperature (at 15 °C) with that in case of MPPT and FL controller, the control methods used lead to an increase in the hydrogen flow up to 57.24 % figs (14.b and 14.c). For more development in total model, variation in ambient pressure is considered to have exactly the correct maximum water temperature with different geographical altitudes (fig. 15).

REFERENCES:

1. Agbli, K.S., Péra, M.C., Hissel, D., Rallières, O., Turpin, C., Doumbia, I., January 2011, Multiphysics simulation of a PEM electrolyser: Energetic Macroscopic Representation approach, *Int. J. of Hydrogen Energy*, vol. 36, n° 2, pp.: 1382 – 1398.
2. Saadi, A., Becherif, M., Aboubou A., Ayad, M.Y., 2012, Static Proton Exchange Membrane Fuel Cell Models Comparison, *Int. Conf. of Elsevier, Energy Conversion and Management*, In Press, DOI: 201210.1016/j.renene.2012.10.012.
3. Becherif, M., Saadi, A., Hissel D., Aboubou, A., Ayad, M.Y., June 2011, Static and dynamic proton exchange membrane Fuel Cell models, *Int. J. of Hydrocarbons Mines and Environmental Research*, ISSN: 2107-6510, Vol. 2, n° 1, pp.: 19-26.
4. http://americanhistory.si.edu/fuelcells/basics.htm
5. Tabanjat, A., Becherif, M., Hissel, D., Hybrid Renewable Energy System connected to the Grid: the Hydrogen Storage Solution, 2012, *Int. Conf. on Renewable Energy: Generation and Applications*, IEEE-ICREGA12, United Arab Emirates.
6. Craig, A., Grimes Oomman, K., Varghese Sudhir Ranjan, Light, water, hydrogen; the solar generation of hydrogen by water photoelectrolysis, 2008, US: Springer, ISBN 978-0-387-33198-0.
7. Solano-Martinez, J., Boulon, L., Hissel, D., Pera, M.-C., Amiet, M., 2009, Energetic macroscopic representation of a multiple architecture heavy duty hybrid vehicle, *Vehicle Power and Propulsion Conference*, VPPC '09 , PP.: 1322 – 1329.
8. Bossmann, T., Bouscayrol, A., Barrade, P., Lemoufouet, S., Rufer, A., 2007, Energetic Macroscopic Representation of a hybridstorage system based on supercapacitors and compressed air, *Int. Conf. on Industrial Electronics*, pp.: 2691 – 2696.
9. Chrenko, D., Péra, M.C., Hissel, D., 4-7 June 2007, Fuel cell modeling and control with Energetic Macroscopic Representation, ISIE 2007. *Int. IEEE. Symposium on Industrial Electronics*, pp.: 169-174. Isbn: 978-1-4244-0755-2.c.
10. Chrenko, D., Coulié, J., Lecoq, S., Péra, M-C., Hissel, D., , 2009, Static and dynamic modeling of a diesel fuel processing unit for polymer electrolyte fuel cell supply, *Int. J. on Hydrogen Energy*, vol. 34, n° 3: PP.: 1324–1335.
11. Chrenko, D., Péra, M.C., Hissel, D., Bouscayrol, A., 2009, Inversion-based control of a proton exchange membrane fuel cell system using energetic macroscopic representation, *Journal of fuel cell science and technology*, vol. 6, n°2, Note(s): 024501.1-024501.5, ISSN 1550-624X.
12. Bouscayrol, A., Delarue, P., Semail, E., Hautier, J., Verhille, J., 2002, Energetic Macroscopic Representation (EMR) application to a system of multimachine traction, *Int. J. of electrical egineering*, vol. 5, n°3-4, MMS representation of VAL 206,[In French].
13. Bouscayrol, A., Davat, B., De Fornel, B., Frannçois, B., Hautier, J.P., Meibody- Tabar, F., Pietrzak-David, M., 2000, Multi-converter multimachine systems: application for electromechanical drives, *The European physical journal applied physics*, vol. 10, n°2, pp.:131-47.
14. http://www.emrwebsite.org/
15. Becherif, M., Ayad, M.Y., Hissel, D., Mkahl, R., 2011, Design and sizing of a stand-alone recharging point for battery electrical vehicles using photovoltaic energy, *Vehicle Power and Propulsion Conference*, *IEEE-VPPC'11*, Chicago, USA, DOI: 10.1109/VPPC.6043075.
16. http://en.wikipedia.org/wiki/Maximum_power_point_tracking
17. Becherif, M., Hissel, D., 2010, MPPT of a PEMFC based on air supply control of the motocompressor group, *Int. J. on Hydrogen Eneergy*, Vol. 35, n° 22, pp.: 12521-12530.
18. Hohm, D. P. Ropp, M. E., 2003, Progress in photovoltaics: research and applications, 22 NOV 2002, *Int. J. on Energy Science and Engineering*, vol. 11, n° 1, pp.: 47-62.
19. Mokri, A., Emziane, M., 20-25 June 2010, Evaluation of a CPV system with beam-splitting for Hydrogen generation, *The 35th IEEE Photovoltaic Specialists Conference*, Hawaii, USA.